

Phase evolution of 17(Cu-10Ni)-(NiFe₂O₄-10NiO) cermet inert anode during aluminum electrolysis

LIU Jian-yuan, LI Zhi-you, TAO Yu-qiang, ZHANG Dou, ZHOU Ke-chao

State Key Laboratory for Powder Metallurgy, Central South University, Changsha 410083, China

Received 7 June 2010; accepted 14 October 2010

Abstract: 17(Cu-10Ni)-(NiFe₂O₄-10NiO) cermets were prepared by cold pressing and sintering in nitrogen atmosphere, and tested as inert anode for aluminum electrolysis at 960 °C for 10 and 40 h, respectively. Microstructures and phase compositions of the as-sintered and post-electrolyzed samples were investigated. The impurity contents in the electrolyte and the cathode metal were detected in order to investigate the corrosion characteristic of the elements of Fe, Ni and Cu in the anode. A dense NiFe₂O₄ layer was observed on the surface of anode and thickened with prolonging the electrolysis time. In the newly formed dense ceramic layer, NiO phase disappeared as a result of being swallowed by NiFe₂O₄ phase, and the metal phase was oxidized during the electrolysis in which Cu element showed a higher dissolution rate than Fe and Ni elements. The formation process of the dense ceramic layer during the electrolysis was presented and explained by using the corrosion mode of the metal phase and the transformation mechanism from NiO phase to NiFe₂O₄ phase.

Key words: inert anode; spinel; phase transformation; aluminum electrolysis

1 Introduction

It has become an urgent goal to replace the conventional consumable carbon anode with an inert or non-consumable anode in Hall-Heroult electrolysis cells for the production of aluminum since the middle of 1980s, in views of technical, commercial and environmental perspectives[1–4]. Nickel ferrite (NiFe₂O₄) based cermets have received a lot of attention as a candidate of inert anode material. Metallic Cu and/or Ni were often utilized as the metal phase to enhance the electrical conductivity and thermal shock resistance, while an appropriate amount of NiO was added to improve the corrosion resistance[1–2]. However, the corrosion process of the cermets became much complicated with the appearance of metal and bunsenite (NiO) phases in NiFe₂O₄ matrix. In general, the corrosion of cermet anode during the electrolysis is mainly due to the leaching of the metal phase and the chemical dissolution of the ceramic phase, and the corrosion products then enter the cathode metal through the reduction process[5]. The leaching mechanism of the

metallic Ni phase was generally attributed to the anodic dissolution during the electrolysis[1]. However, arguments existed for Cu and Cu-riched Cu-Ni alloy. TARCY[1] explained that the metal phase was oxidized first and then dissolved, while OLSEN et al[6–8] concluded that the metal phase was dissolved directly.

Similarly, there were disputes about the effects of NiO content on the corrosion resistance. DUAN[9] reported that the increase of NiO content in ceramic phase reduced the Fe concentration in electrolyte, yet had little effect on the Ni concentration in the Na₃AlF₆-10%AlF₃-5%CaF₂-5% Al₂O₃ melts at 960 °C. ALCOA (Aluminum Company of America) reported that NiFe₂O₄-18NiO-17Cu cermet had the best electrical conductivity and corrosion resistance among a series of NiFe₂O₄-based cermets with different contents of Cu and NiO[1–2]. Based on the optimal composition of ALCOA's, OLSEN and THONSTAD[6–7] analyzed the corrosion behavior of NiFe₂O₄-based cermet through 4 h and 50 h electrolysis tests, respectively. In their experiments, the amounts of excess NiO were varied by 0, 17%, and 23% in the composition, and the amount of metal phase was adjusted to 20% by introducing

Foundation item: Project (2005CB623703) supported by the National Basic Research Program of China; Project (50721003) supported by the National Natural Science Fund for Innovation Group of China; Project (2008AA030501) supported by the National High-Tech Research and Development Program of China

Corresponding author: LI Zhi-you; Tel: +86-731-88830464; E-mail: lizhiyou@mail.csu.edu.cn
DOI: 10.1016/S1003-6326(11)60752-8

additional 3% Ni. The contents of NiO showed little benefit to the corrosion resistance, and even resulted in a detrimental effect in the 4 h electrolysis test[6]. However, LI et al[10–11] later reported that a moderate content of NiO would contribute to the increase of the sintering density and the corrosion resistance of NiFe_2O_4 -based cermets with nickel as the metal phase, particularly for the composition of NiFe_2O_4 -10NiO. However, the mechanisms are still not clear about the origin of the discrepancy in the effects of NiO phase on the corrosion performance of NiFe_2O_4 -based cermets under similar electrolytic conditions.

In order to clarify the situation and find a suitable inert anode material, 17(Cu-10Ni)-(NiFe₂O₄-10NiO) cermets were prepared in the present work and employed in laboratory-scale electrolysis tests under a similar electrolytic condition in Refs.[10–11] for 10 h and 40 h, respectively. The transformations in the microstructure and the composition of the metal and NiO phases during the electrolysis were presented in details.

2 Experimental

2.1 Fabrication of NiFe_2O_4 -based cermet

NiFe_2O_4 -10NiO ceramic was synthesized from commercial NiO (77.64% Ni, mass fraction, <147 μm , Jinchuan Group Ltd.) and Fe_2O_3 (99.60 %, 0.75 μm , low-silica grade, JFE Chemical Co.) powders. NiO and Fe_2O_3 powders were ball milled for 10 h in zirconia media using ethanol as the solvent. The dried mixture was calcined at 1 200 °C for 4 h in air, and followed by further ball milling for 24 h. Cu-10Ni powders were prepared by chemically coating Ni on Cu powder(99.5%, 9.86 μm , Gripm Advance Materials Co.). The ceramic and metal powders were then mixed with a mass ratio of 83:17 and ball milled for 4 h in water containing 1.2% PVA. The dried powders were pressed at 200 MPa to form cylindrical blocks ($d20\text{ mm}\times H40\text{ mm}$). Sintering was performed at 1 300 °C for 4 h in N_2 atmosphere with original oxygen partial pressure of $\sim 100\text{ Pa}$ using a heating rate of 1.4 °C/min and cooling rate of 1 °C/min.

2.2 Electrolysis process

Fig.1 shows the sketch map of the electrolysis cell. 350 g reagent ($\text{CR}=n(\text{NaF})/n(\text{AlF}_3)=2.3$) comprising of 5% CaF_2 and 7.43% Al_2O_3 was employed as the electrolyte. 68 g pure Al was placed in the bottom of the cell as the cathode. The anode samples were lapped first to remove the surface of $\sim 0.5\text{ mm}$ in thickness and then glued to a guide rod (316 stainless-steel) by a high-temperature conductive adhesive. The assembled electrolysis cell was put into a vertical furnace and heated to 960 °C for electrolysis. A distance of 3 cm was

used between anode and cathode, and a current density of 1.0 A/cm^2 was adjusted based on the bottom area of anode. Al_2O_3 powders were added to the cell every 30 min using the amount based on the electrolytic consumption rate at 80% cathode current efficiency. After the electrolysis, the anode was sectioned along axial direction and polished for further analysis. Electrolyte and cathode metal were collected for impurities analysis. The mass increments of Fe, Ni and Cu elements were calculated from their contents in the pre- and post-test electrolyte and cathode metal respectively.

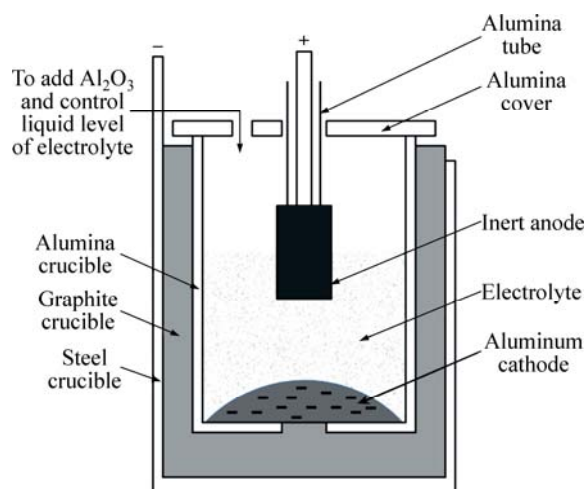


Fig.1 Schematic structure of electrolysis cell

2.3 Characterization

The bulk densities of sintered samples were tested using the Archimedes' method. The microstructures were examined by scanning electron microscope (SEM) (JSM-6360LV, JEOL), and the element contents and distributions were analyzed by energy dispersive spectroscopy (EDS) using the mean results at five different points. The impurity amount in the cathode and the electrolyte were detected by inductive coupled plasma (ICP) (IRIS Advantage 1000) and X-ray diffraction fluorescence analyzer (XRF) (Philips PW2424), respectively.

3 Results and discussion

3.1 Microstructural evolution

Fig.2 shows the SEM photograph of a sintered sample with the relative density of 98.2%. NiFe_2O_4 spinel phase exhibited grain sizes of 30–40 μm . NiO and metal phases distributed along the grain boundary of NiFe_2O_4 phase as irregularly shaped particles. Some holes existed along the grain boundaries and phase boundaries. The compositions of the three phases, NiFe_2O_4 , NiO and metal, in the as-sintered sample are listed in Tables 1 and 2. The metal phase contained

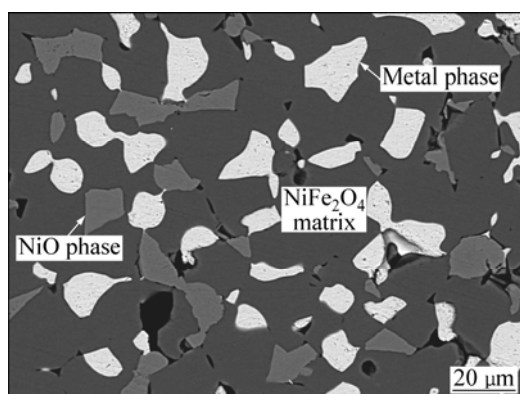


Fig.2 SEM photograph of as-sintered 17(Cu-10Ni)-(NiFe₂O₄-10NiO) cermet

4.29% (molar fraction) Fe and 25.10% (molar fraction) Ni. The content of Ni in this metal phase was much higher than that in the original Cu-Ni metal powder, which was 10% (mass fraction). NiO phase contained 8.29% Fe. The molar ratio of Fe to Ni in NiFe₂O₄ phase was 2.91, much higher than the theoretical value of 2. Similar phenomena of the increase of Ni content in the metal phase and the existence of Fe element in NiO phase were also reported by ALCOA[2] and OLSEN and THONSTAD[6]. These were attributed to either the exchange reaction among Cu, NiO and NiFe₂O₄[2], or the thermal reduction by residual carbon and the decomposition products of the organic solvent and additives[6]. Another possible explanation for a high Fe content in NiO phase can be the solution of NiFe₂O₄ in NiO phase during the sintering process. The solubility of Fe element in NiO phase increases with lowering the oxygen partial pressure and raising the temperature in Fe₂O₃-NiO pseudo-binary system. The molar ratio of Fe to (Ni+Fe) in NiO phase can rise up to 0.2 at 1 300 °C in

air[12]. As a great quantity of iron oxides dissolve in NiO phase at high temperature, the precipitation of NiFe₂O₄ spinel phase may become incomplete if cooling quickly. An elongated heating treatment and a slow cooling rate could encourage the growth of the spinel precipitate in NiO phase[13].

Fig.3(a) shows a distinct layer of ~30 μm in thickness formed on the surface of anode after 10 h electrolysis, indicating no trace of any metal phase. This metal-free surface layer was termed as “metal-lost layer” in this work. Similar to the previous report[7], the formation of the metal-lost layer was not just the result of the dissolution of the metal grains exposed to the electrolyte leaving the ceramics matrix behind. Inside this layer, NiO grains became more irregular, and boundaries between NiO and NiFe₂O₄ phases became closer than those in Fig.2. The NiO phase exhibited a trace of fragment and the spinel precipitates appeared clearly inside NiO grains, as shown in Figs.3(b) and (c). It was found out that NiO phase was swallowed by NiFe₂O₄ phase. A gray substance with the brightness similar to NiO phase formed on the periphery of the metal phase. On the outer surface, both NiO and metal phases were not exposed directly to the electrolyte and instead covered by NiFe₂O₄ phase.

Fig.4 shows the microstructures of the polished cross-sections near the surface and the core part of an anode sample after electrolysis for 40 h. Compared with the anode sample after electrolysis for 10 h, the thickness of the metal-lost layer increased to ~150 μm, and became denser than the anode material itself. Inside the metal-lost layer, NiO phase disappeared as well. This is the first time of such an observation on the disappearance of NiO phase inside the metal-lost layer. OLSEN and THONSTAD[7] reported NiO phase still existed in a 50 μm-thick metal-lost layer after electrolysis for 50 h, and

Table 1 Element contents and Ni to Cu molar ratio in metal phase and gray substance in as-sintered and 10 h-electrolyzed samples

Sample	Element	$x(\text{Cu})/\%$	$x(\text{Ni})/\%$	$x(\text{Fe})/\%$	$x(\text{O})/\%$	$n(\text{Ni}):n(\text{Cu})$
As-sintered	Metal phase	66.68	25.10	4.29	3.93	0.376
	Gray substance	68.18	10.41	6.00	15.41	0.147
Electrolysis for 10 h	Metal phase	61.61	29.14	5.54	3.71	0.473

Table 2 Element contents and Fe to Ni molar ratio in NiO and NiFe₂O₄ phases in as-sintered and 10 h-electrolyzed samples

Phase	Position	$x(\text{O})/\%$	$x(\text{Fe})/\%$	$x(\text{Ni})/\%$	$x(\text{Cu})/\%$	$n(\text{Fe}):n(\text{Ni})$
NiO	As-sintered	44.32	8.29	46.86	0.53	0.177
	10 h electrolysis	In core	44.89	8.94	45.51	0.66
		Near surface	42.79	7.26	49.36	0.147
	As-sintered	51.96	35.77	12.28	—	2.910
NiFe ₂ O ₄	10 h electrolysis	In core	51.96	35.24	12.45	0.25
		Near surface	49.88	35.31	14.33	0.48

Selected phases in core area were about 500 μm far from the outer surface, and those near surface were in the metal-lost layer.

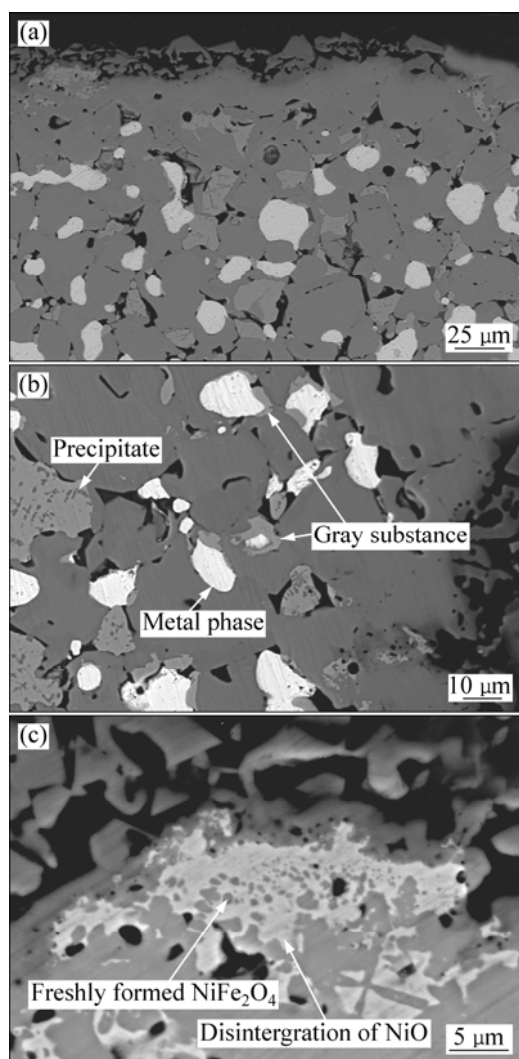


Fig.3 SEM photographs of anode sample after electrolysis at 960 °C for 10 h: (a) Cross-sectional view of outer layer; (b) Microstructure near surface; (c) Magnified microstructure of upper left corner in (a)

suggested the densification of the metal-lost layer resulted mainly from the formation of aluminates such as FeAl_2O_4 .

The contents of the gray substance showed a clear discrepancy in the three types of samples, i.e. the outer layer of a 10 h-electrolyzed sample, the core area of a 40 h-electrolyzed sample and the as-sintered sample, with an order of contents from the high to the low, as shown in Fig.3(b), Fig.4(b) and Fig.2, respectively. In the outer layer of a 10 h-electrolyzed sample, EDS analysis was performed on the gray substance and the metal phase in the areas of 30–50 μm away from the surface. Table 1 presents the EDS analysis results. In the gray substance, the oxygen content increased and the molar ratio of Ni to Cu decreased compared with the metal matrix. But the oxygen content in the metal phase decreased only slightly compared with that in the as-sintered sample.

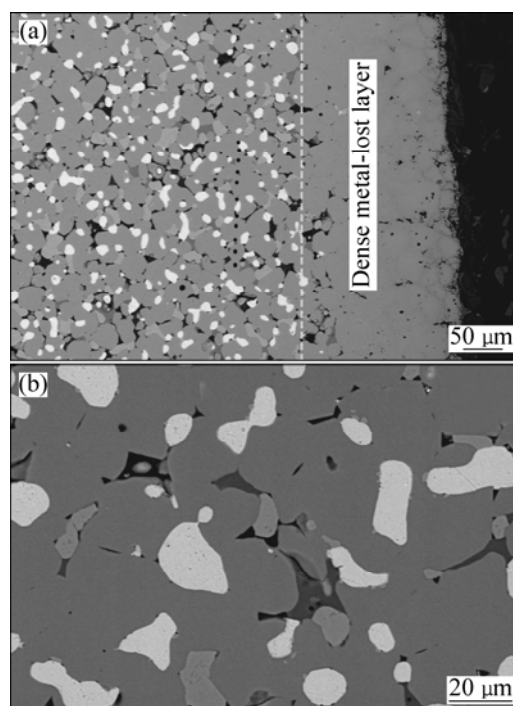


Fig.4 SEM photographs of anode sample after electrolysis at 960 °C for 40 h: (a) Cross-sectional view of dense ceramic layer formed on outer surface; (b) Microstructure of core area

Since the gray substance with high oxygen content decreased in the core area of the 40 h-electrolyzed sample. It is clear that the gray substance was mainly derived from the oxidation of the metal phase, especially for the copper element. The gray substance on the periphery of the metal phase was also found after the oxidation of a cermet of a similar composition at high temperature, but was characterized as nickel oxides[13].

NiO grains exhibit a similar morphology in the core part of the 40 h-electrolyzed sample and in the as-sintered sample, as shown in Fig.4(b) and Fig.2, respectively. Spinel precipitates in the NiO phase were indistinct, less evident than those in the outer layer of the 10 h-electrolyzed sample, as shown in Fig.3(b). This indicates the protective functions of both the dense sintered part and the pore-free metal-lost layer to block the matter exchanges between the NiO phase and the environmental media such as air and the electrolyte during the electrolysis. On the contrary, the matter exchanges became inevitable for areas close to the surface of anode during the electrolysis via three possible mechanisms: 1) the diffusion of the atomic oxygen generated by the anodic reaction; 2) the infiltration of the molten electrolyte; and 3) the dissolution of the compositional elements of the anode. These finally induced the growth of spinel precipitates in the NiO grains which located near the surface of anode and the densification of the metal-lost layer.

3.2 Compositions of ceramics phases in metal-lost layer

Table 2 presents the compositions of NiFe_2O_4 and NiO phases in the metal-lost layer and the core part after electrolysis for 10 h. The contents of oxygen and Fe elements in the NiO phase became less in the metal-lost layer than those in the core region, and the same tendency existed for the oxygen content and Fe to Ni molar ratio in NiFe_2O_4 phase. Since the peaks of Al, F and other elements from the electrolyte were unobvious in the EDS spectra, the compositional changes in NiO and NiFe_2O_4 phases were not induced by the reactions between the ceramic phases and the electrolyte, but mainly attributed to the diffusion reaction between NiO and NiFe_2O_4 phases in the formation of the dense ceramics layer, which could be confirmed by the fact that NiO phase was swallowed by NiFe_2O_4 phase, as shown in Fig.3(c).

Table 3 shows the compositions of the metal-lost layer formed in the 40 h-electrolyzed sample and the NiFe_2O_4 phase in the core area. In comparison with the results of 10 h-electrolyzed sample, the Fe to Ni molar ratio of NiFe_2O_4 phase in the metal-lost layer became further reduced. Besides the compositional elements in the as-sintered sample, Al element appeared in the metal-lost layer of 40 h-electrolyzed sample. Al content was rather high in the surface area but became low in the inner part. Since the characteristic peaks of F, Na and other electrolyte elements were unobvious in EDS analysis, the appearance of Al element in the dense metal-lost layer resulted from the reaction of the ceramic phases in the cermet with Al_2O_3 dissolved in the electrolyte [8, 14], not from the infiltration of the molten electrolyte. Followed by the dissolutions of the NiO and NiFe_2O_4 phases in the electrolysis, some aluminates such as NiAl_2O_4 and FeAl_2O_4 [8, 14] would be generated and deposited on the outer surface of the anode. The aluminates and NiFe_2O_4 phase can form solid-state solution due to the same crystallographic structure. Al

element showed a concentration gradient in the dense metal-lost layer from the outer part to the inner part, indicating a concentration-controlled diffusion mechanism for Al element.

As presented in Table 3, Cu content increased in the dense ceramic layer, which was still much lower than that of the as-sintered sample, i.e. 0.18 calculated from $n(\text{Cu}):n(\text{Fe}+\text{Ni}+\text{Cu})$. Although the Fe to Ni molar ratio in the dense ceramic layer after electrolysis for 40 h was slightly lower than that in the NiFe_2O_4 phase near the surface of 10 h-electrolyzed sample, as shown in Tables 3 and 2 respectively, the former was still higher than the nominal value of 1.39 based on its composition of 17(Cu-10Ni)-(NiFe₂O₄-10NiO). The results suggest that Cu and Ni among the metal elements in the outer surface can diffuse into the electrolyte at a higher rate, resulting in the changed ratios among the metal elements in the dense ceramic layer.

The impurity contents in the cathode and the electrolyte after electrolysis for 40 h were detected in order to further investigate the dissolution discrepancy of metal elements from the anode. Table 4 presents the net increase of the amount of the metal elements in the electrolyte and the cathode. The mass ratio of Cu to the total metal elements corroded from the anode was 0.34, higher than the nominal value of 0.197 in the as-sintered sample calculated based on the powder mixtures. The mass ratio of Fe to Ni was equal to the nominal value of 1.32. This suggested Cu element was prior to corrosion in the electrolysis, which was confirmed by the results of the element contents in the dense ceramics layer, as listed in Table 3. Ni and Fe elements showed little corrosion difference in the electrolysis, which did not hold with the composition analysis results of the dense metal-lost layer. However, the discrepancy existed for the analysis of Fe to Ni molar ratio in the electrolyte and the cathode. The increase of Fe content and the decrease of Ni content were due to two possible sources. On one side, the additional Fe impurity can originate from the

Table 3 Element contents, Fe to Ni and Cu to Fe+Ni+Cu molar ratios in NiFe_2O_4 phase in different areas of 40 h-electrolyzed sample

Distance from outer surface/ μm	$x(\text{O})/\%$	$x(\text{Fe})/\%$	$x(\text{Ni})/\%$	$x(\text{Cu})/\%$	$x(\text{Al})/\%$	$n(\text{Fe}):n(\text{Ni})$	$n(\text{Cu}):[n(\text{Fe})+n(\text{Ni})+n(\text{Cu})]$
>500	52.87	34.89	12.24	0.26	—	2.85	0.005 5
40–60	50.64	32.92	14.84	0.67	0.92	2.22	0.013 8
10–20	50.00	32.21	14.18	0.67	2.67	2.27	0.014 2

Table 4 Net increments and mass ratio of impurities in electrolyte and cathode after electrolysis for 40 h

Sample	$m(\text{Fe})/\text{g}$	$m(\text{Ni})/\text{g}$	$m(\text{Cu})/\text{g}$	$m(\text{Fe}):m(\text{Ni})$	$m(\text{Cu}):[m(\text{Fe})+m(\text{Ni})+m(\text{Cu})]$
In electrolyte	0.038	0.049	0.054	0.78	0.38
In cathode	0.091	0.046	0.063	1.98	0.32
Total	0.129	0.095	0.117	1.36	0.34

Net increment means the content after test minus the initial content.

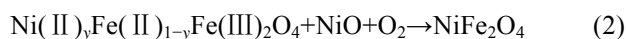
crucible and the alumina feed during the electrolysis[7]. On the other side, the evaporation of the electrolyte may lead to a quicker loss of Ni element than Fe element after the dissolution in the electrolyte, as pointed out in previous reports that the contents of Ni and Cu were higher in the upper electrolyte bath and Fe content was higher in the bottom part[15–16].

3.3 Densification of metal-lost layer

The Cu-Ni metal phase may be corroded successively through two mechanisms, i.e., anodic dissolution[7] and the oxidation followed by dissolution[1]. In the electrolysis process, the dissolution or oxidation of the metal phase in cermets may be determined by whether the metal phase has direct contact with the electrolyte melt. Before the formation of the dense ceramics layer on the surface of anode, especially in the initial stage, the metal grains in contact with the electrolyte were subjected to the anodic dissolution due to their electrochemically unstable nature under anodic polarization. This corrosion mode was supported by the fact that no trace of the metal grain was observed at the interface of the anode and the electrolyte, as shown in this work and other reports[7]. The formation of the dense ceramic layer hindered the anodic dissolution of the metal phase as it functioned as the blocking layer between the metal phase and the electrolyte.

The other corrosion mode considered the diffusion of the atomic oxygen generated by anodic reaction into the interior through the ceramic layer, resulting in the oxidization of the metal phase as being described by TARCY[1]. The corrosion rate of the metal phase reduced consequently alongside the electrolysis, while the metal elements in the oxidized products need to diffuse across the dense ceramics layer. As reported by OLSEN and THONSTAD[7], the dissolution rate of Cu element became very low after a dense layer has formed through pre-electrolysis. Its chemical mass transfer coefficient reduced by nearly three orders of magnitude, and was 1–2 orders of magnitude lower than that of Fe, Ni elements[7].

Unlike the results reported by OLSEN and THONSTAD[7] that the composition of the oxide phases and the relative amounts of Ni and Fe in each oxide were stable and unchanged from the interior to the outer surface during the electrolysis, the diffusion reactions between NiO and NiFe₂O₄ phases in the electrolysis were observed in this study. The reactions may be related to the existence of Fe²⁺ in both ceramic phases. The stoichiometric formulas of NiO and NiFe₂O₄ phases in the as-sintered samples are Ni(II)_xFe(II)_{1-x}O and Ni(II)_yFe(II)_{1-y}Fe(III)₂O₄, respectively. Under the action of nascent oxygen from the anodic reaction, Fe²⁺ was oxidized to Fe³⁺, as shown below:



Reaction (1) led to the growth of small NiFe₂O₄ precipitates in NiO phase. Reaction (2) promoted the movement of the interfaces between NiO and NiFe₂O₄ phases towards NiO phase. Both reactions resulted in the decrease of NiO grain size.

The formation of the dense metal-lost layer was caused mainly by the transformation of NiO phase and the oxidation of the metal phase. At the beginning of electrolysis, the metal phase in the outer surface was anodically dissolved, and some NiO grains uncovered by NiFe₂O₄ phase were chemically dissolved. Meanwhile, atomic oxygen was generated at the corrosion-resistant NiFe₂O₄ phase via the anodic reaction, and diffused through the NiFe₂O₄ phase, resulting in the transformation of NiO phase to NiFe₂O₄ phase and the oxidation of the covered metal phase. The products can fill the initial holes in as-sintered microstructure and secondary holes generated by the selective dissolution of Cu and Ni elements, since volume expansion can be both induced by the transformation of higher density phase NiO (6.81 g/cm³) to lower density phase NiFe₂O₄ (5.37 g/cm³), and the oxidation of the higher density metal phase to the lower density oxides. In addition, the deposition of Al₂O₃ and the reaction of Al₂O₃ with the initial ceramic [8, 14] can also fill the holes in the outer surface. After the formation of the corrosion-resistant stable ceramic dense layer, the corrosion rate of anode reduced, while the transformations of the NiO phase and the metal phase continued. The dense ceramic layer thickened and extended towards the inner part with the increase of electrolysis time, although it dissolved slowly as well. The dense ceramic layer would contribute to hindering the quick leaching of the metal phase and function as a corrosion-resistant stable surface in electrolysis[7]. It is still uncertain whether the thickening phenomenon of the dense ceramic layer will continue or finally reach an equilibrium state in the electrolysis process. Further work is currently under investigation and more results will be presented later, together with the characterizations of conductivity and dielectric properties of the ceramic dense layer.

4 Conclusions

1) 17(Cu-10Ni)-(NiFe₂O₄-10NiO) cermets were employed as the inert anode in laboratory-scale aluminum electrolysis tests for 10 h and 40 h. Microstructural evolution and compositional analysis of as-sintered, 10 h- and 40 h-electrolyzed samples, together with the impurity analysis of the electrolyte and the cathode metal, revealed the correlation between the

anode phases and the corrosion during the electrolysis process.

2) A dense metal-lost ceramic layer was gradually formed in the surface layer of 17 (Cu-10Ni) - (NiFe₂O₄-10NiO) cermet during the electrolysis in nearly alumina-saturated sodium cryolite molten salt system at 960 °C. The formation of the dense ceramic layer was mainly attributed to the transformation of NiO phase, the oxidation of the metal phase, and the deposition of aluminates.

3) The copper-nickel metal phase was oxidized in the electrolysis after the formation of dense ceramic layer on the surface. Cu element in the dense layer was easier to dissolve into the electrolyte than Fe and Ni elements.

4) The disappearance of NiO phase and the transformation to the spinel phase were due to the growth of NiFe₂O₄ precipitates in NiO phase and the combination reaction between NiFe₂O₄ and NiO under the role of nascent oxygen from the anodic reaction.

References

- [1] TARCY G P. Corrosion and passivation of cermet inert anodes in cryolite-type electrolytes [C]//MILLER R E. Light Metals. Warrendale, PA: TMS, 1986: 309–320.
- [2] WEYAND J D, DEYOUNG D H, RAY S P, TARCY G P, BAKER F W. Inert anodes for aluminium smelting [R]. Washington D C: Aluminium Company of America, 1986.
- [3] PAWLEK R P. Inert anodes: An update [C]//de YOUNG D H. Light Metals. Warrendale, PA: TMS, 2008: 1039–1045.
- [4] de NORA V, NGUYEN T. Inert anodes: challenges from fundamental research to industrial application [C]//BEARNE G. Light Metals. Warrendale, PA: TMS, 2009: 417–421.
- [5] XIAO H, HOVLAND R, ROLSETH S, THONSTAD J. Studies on the corrosion and the behaviour of inert anodes in aluminium electrolysis [J]. Metall Mater Trans B, 1996, 27(2): 185–193.
- [6] OLSEN E, THONSTAD J. Nickel ferrite as inert anodes in aluminium electrolysis: Part I: Material fabrication and preliminary testing [J]. J Appl Electrochem, 1999, 29(3): 293–299.
- [7] OLSEN E, THONSTAD J. Nickel ferrite as inert anodes in aluminium electrolysis: Part II: Material performance and long-term testing [J]. J Appl Electrochem, 1999, 29(3): 301–311.
- [8] LORENTSEN O, THONSTAD J. Electrolysis and post-testing of inert cermet anodes [C]//SCHNEIDER W G. Light Metals Warrendale, PA: TMS, 2002: 137–143.
- [9] DUAN Hua-nan N. On the electrolytic corrosion behavior of Cu-Ni-NiO-NiFe₂O₄ cermets in cryolite-alumina melts [D]. Changsha: School of Metallurgy Science and Engineering, Central South University, 2005: 36–45. (in Chinese)
- [10] LI Jie, DUAN Hua-nan, LAI Yan-qiang, TIAN Zhong-liang, LIU Ye-xiang. Effect of NiO content on corrosion behaviour of Ni-xNiO-NiFe₂O₄ cermets in Na₃AlF₆-Al₂O₃ melts [J]. Trans Nonferrous Met Soc China, 2004, 14(6): 1180–1186.
- [11] LAI Y Q, DUAN H N, LI J, SUN X G, LIU Y X. On the corrosion behaviour of Ni-NiO-NiFe₂O₄ cermet as inert anodes in aluminum electrolysis [C]//KVANDER H. Light Metals. Warrendale, PA: TMS, 2005: 529–534.
- [12] RHAMDHANI M A, HAYES P C, JAK E. Subsolidus phase equilibria of the Fe-Ni-O system [J]. Metallurgical and Materials Transactions B, 2008, 39: 690–701.
- [13] RIOULT F, PIJOLAT M, VALDIVIESO F, PRIN-LAMAZE M A. High-temperature oxidation of a Cu-Ni based cermet: Kinetic and microstructural study [J]. J Am Ceram Soc, 2006, 89(3): 996–1005.
- [14] ZHANG Lei, JIAO Wan-li, YAO Guang-chun. Preparation of NiFe₂O₄ inert anode and its electrolysis corrosion mechanism [J]. Journal of the Chinese Ceramic Society, 2005, 33(12): 1431–1436. (in Chinese)
- [15] PIETRZYK S, OBLAKOWSKI R. Investigation of the concentration of the inert anodes in the bath and metal during aluminum electrolysis [C]//PIETRZYK Y. Light Metals. Warrendale, PA: TMS, 1999: 407–411.
- [16] WANG J W, LAI Y Q, TIAN Z L, LI J, LIU Y X. Investigation of 5Cu-(10NiO-NiFe₂O₄) inert anode corrosion during low-temperature aluminum electrolysis [C]//SOLLIE M. Light Metals, Warrendale, PA: TMS, 2007: 525–530.

17(Cu-10Ni)-(NiFe₂O₄-10NiO)基金属陶瓷 在铝电解过程中的相演变

刘建元, 李志友, 陶玉强, 张 斗, 周科朝

中南大学 粉末冶金国家重点实验室, 长沙 410083

摘 要: 采用冷压气氛烧结制备 17(Cu-10Ni)-(NiFe₂O₄-10NiO)金属陶瓷, 并作为阳极在 960 °C 下分别进行 10 和 40 h 的铝电解试验。对电解前后金属陶瓷的显微结构、物相成分进行分析检测。对电解质及阴极金属中的杂质含量进行分析, 研究阳极组成中 Fe、Ni 和 Cu 元素的腐蚀行为。研究发现: 在电解过程中, 在材料表面形成 NiFe₂O₄ 相致密层, 该致密层随电解时间的延长而增厚。在 NiFe₂O₄ 相致密层形成与增厚过程中, 出现 NiFe₂O₄ 相吞噬 NiO 相和金属相氧化的现象, 金属陶瓷中 Cu 元素优先腐蚀溶解。并着重讨论 NiFe₂O₄ 相致密层形成与增厚过程中金属相的腐蚀形式及 NiO 相向 NiFe₂O₄ 相的转变机制。

关键词: 惰性阳极; 尖晶石; 相转变; 铝电解

(Edited by YANG Hua)